

# Metabolomics Profiling of *Rhodomyrtus tomentosa* (Ait.) Hassk. Leaves and Fruits Using $^1\text{H}$ NMR Spectroscopy

Evi Mintowati Kuntorini <sup>1,2\*</sup>, Laurentius Hartanto Nugroho <sup>1</sup>,

Maryani Maryani <sup>1</sup> and Tri Rini Nuringtyas <sup>1,3\*</sup>

<sup>1</sup>Faculty of Biology, Universitas Gadjah Mada. Teknika Selatan Street, 55281, Yogyakarta, Indonesia

<sup>2</sup>Departement of Biology, Faculty of Mathematics and Natural Sciences, Universitas Lambung

Mangkurat. A. Yani Km. 36 Street, Banjarbaru City, 70714, South Kalimantan, Indonesia

<sup>3</sup>Research Center for Biotechnology, Universitas Gadjah Mada, Teknika Utara stree, 55281, Yogyakarta, Indonesia

(Received July 26, 2023; Revised September 27, 2023; Accepted September 29, 2023)

**Abstract:** Several investigations are extensively documenting the presence of metabolites with antibacterial, anticancer, antioxidant, and anti-inflammatory properties in extracts derived from *Rhodomyrtus tomentosa* fruits and leaves. Therefore, this study aimed to evaluate the metabolite profile of *R. tomentosa* fruits and leaves at various maturity stages and determine their phytomedicinal values.  $^1\text{H}$  NMR and chemometric analyses were used to conduct a metabolomics study for comparing the metabolite profile and phytomedicinal values of different plant organs at varying ages. Leaves were classified into young and old categories, while fruits were divided into three maturity stages, namely green, red, and purple. The wild-grown fruits and leaves of *R. tomentosa* (Ait.) Hassk were gathered in Banjarbaru, South Kalimantan Province, Indonesia. The results of multivariate analysis showed that choline, methionine, mannitol, and  $\beta$ -glucose compounds were three times higher in fruits compared to leaves. Meanwhile, the concentration of aspartate, myricetin, and quercetin compounds was three times higher in leaves compared to fruits. The quantities of secondary metabolites, including flavonoids, were higher in young leaves and green fruits than in old, red, and purple fruits.

**Keywords:** *Rhodomyrtus tomentosa*; flavonoid;  $^1\text{H}$ -NMR; multivariate statistical analysis. © 2023 ACG Publications. All rights reserved.

## 1. Introduction

Plants are significantly important in the daily lives of people by providing essential resources such as medicine, food, fiber for clothing, and wood for building. Among these resources, plants used for treating different medical conditions are considered the most valuable. Individuals without access to modern healthcare still place great value on traditional medical practices. Several studies have shown that the majority of traditional medicines are produced from plant-based materials. A recent report stated that approximately 80% of the global population relies on plants to treat a wide range of ailments, indicating their widespread usage. Consequently, herbal medicines have become integral components of modern therapy, with 25% of medications available worldwide originating from plants [1].

---

\* Corresponding author: E-Mail: [evimintowati@ulm.ac.id](mailto:evimintowati@ulm.ac.id) ; Phone: +85228952178 ; [tririni@ugm.ac.id](mailto:tririni@ugm.ac.id) ; Phone : +82110117807

## Metabolomics profiling of *Rhodomyrtus tomentosa*

*Rose myrtle*, scientifically known as *Rhodomyrtus tomentosa*/R. *tomentosa* (Ait.) Hassk. is a blossoming plant belonging to the Myrtaceae family. According to previous reports, *R. tomentosa* is indigenous to southern and southeastern Asia, with its natural habitat spanning from India, southern China, the Philippines, and Malaysia, to Sulawesi. This plant has an exceptional ability to grow in various environments, ranging from sea level to elevations of 2400 m. Furthermore, it thrives in diverse locations, including natural forests, beaches, wetlands, riparian zones, moist, wet woods, and bog borders, requiring intense sunlight and minimal soil conditions [2-4]. In tropical and subtropical gardens, *R. tomentosa* is a well-liked ornamental plant, cultivated for its abundant blooms, delectable, and edible fruits. These fruits are often used for several culinary applications, such as pies, salads, and jams, including additional processing into wine, jellies, or canned fruits in Vietnam and China [2]. Modern pharmacological studies have shown that *R. tomentosa* components possess diverse properties, namely antibacterial [5], anticancer [6], anti-inflammatory [7], and antioxidant [8]. Traditional Malaysian, Chinese, and Vietnamese medicine has used its leaves, roots, buds, and fruits for medicinal purposes [4]. For example, the Dayak and the Paser local tribes in East Kalimantan, Indonesia, use the roots to treat diarrhea and stomachaches, and as a postpartum tonic [9]. The crushed leaves serve as external poultices and the tar obtained from its wood is used for eyebrow darkening. These traditional applications are in line with the effects observed in modern pharmacological studies. Several phytochemical reports showed that the plant contains flavonoids, triterpenoids, phenols, microelements, and meroterpenoids [2]. Among these compounds, rhodomyrtone is the most prominent, possessing numerous potential pharmacological properties [10], while piceatannol serves as the main and highly effective phenolic component [3].

In a previous study, the total phenolic content, antioxidant capacity, total flavonoids, and compound distribution in *R. tomentosa* were explored using histochemical analysis [11]. This report did not examine the specific antioxidant profile of fruits and leaves at various stages of development. To address the limitation, <sup>1</sup>H-NMR was used to analyze the metabolite profile in leaves and fruits. Therefore, this study aimed to analyze the secondary and primary metabolites of various parts of *R. tomentosa*, specifically fruits and leaves. The existence of these compounds was correlated with the previously reported bioactivity and phytomedicinal qualities. NMR spectroscopy and multivariate data analysis without chromatographic separation were used to identify metabolites directly from the samples. A metabolic analysis was also conducted on *R. tomentosa* fruits and leaves at various stages of maturation. Subsequently, multivariate statistics were used to determine the compounds significantly contributing to the variations between both parts. This study is the first systematic examination of *R. tomentosa* fruits and leaves at various stages of maturity using a combined NMR and multivariate statistical method. Analysis showed the applicability of the NMR-based method in plant metabolomics.

## 2. Materials and Methods

### 2.1. Plant Materials

In this study, *R. tomentosa* plant was obtained from its natural habitat in the wild. The samples were collected from Banjarbaru, South Kalimantan, Indonesia (3°29'0"S, 114°52'0"E) in August-October 2020. To accurately characterize the plant tissues, Munsell Color Charts were used as a reference guide for samples of leaves and fruits [12]. Leaves samples were selected from young leaves (2<sup>nd</sup> – 6<sup>th</sup> order from the shoot [Munsell Color Charts guide: 5GY (7/8-6/8)]) and old leaves (7<sup>th</sup> -12<sup>th</sup> order from the shoot [Munsell Color Charts guide: 2.5G (4/4-3/4)]). Furthermore, fruit samples used were green [Munsell Color Charts guide: 2.5GY (7/8-6/10)], red [Munsell Color Charts:10R (6/10-5/10)], and purple [Munsell Color Charts:5RP (4/4-3/2)] with a color guide using Munsell Color Charts for Plant tissues, as illustrated in Figure 1A. Subsequently, three replicates of each leaves and fruits were analyzed, followed by identification using the Herbarium Bogoriense, Indonesian Institute of Sciences, located in Bogor, Indonesia, under certificate number 1007/IPH.1.01/If.07/IX/2020.

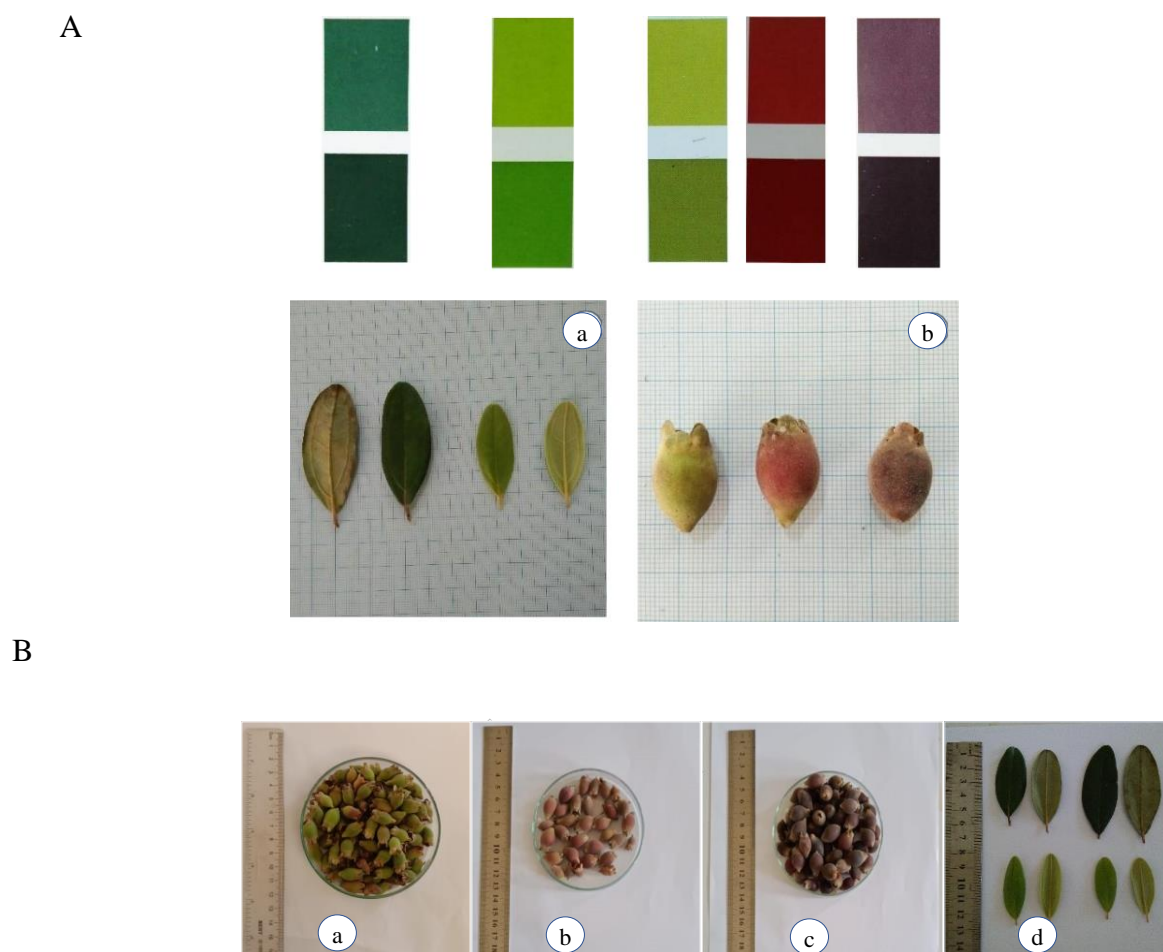


**Figure 1.** *Rhodomyrtus tomentosa* (Ait.) Hassk. (A) a: leaves, b. fruits, with a color guide using Munsell Color Charts for Plant tissues (B) a: green fruits, b: red fruits, c: purple fruits, d: young and old leaves.

## 2.2. Crude Extract Preparation and Sample Preparation for $^1\text{H-NMR}$

The old and young leaves were carefully selected from the tip shoots of *R. tomentosa*, and fruits were dried in an oven at 40 °C, and ground at room temperature. Each grounded material of 500 g was macerated in ethanol of 1000 mL (SmartLab, Indonesia) for 24 h. The solvent was discarded and changed every 24 h, with this process being repeated three times [9,11]. Furthermore, extracts from the same samples were combined, properly mixed, filtered to eliminate cell debris, and dried using a rotary evaporator.

$^1\text{H-NMR}$  sample preparation was carried out using a slightly modified version of the sample extraction of previously reported methods [15]. Precisely, 25 mg of the crude extract was placed into a 2 mL Eppendorf tube along with 1 mL of NMR solvent, comprising 0.5 mL of methanol- $\text{d}_4$ , 0.5 mL of  $\text{KH}_2\text{PO}_4$  buffer, and pH 6.0 containing 0.001% TMSP (trimethyl silypropionic acid sodium, Sigma-Aldrich). The mixture was vortexed, sonicated for 1 min, homogenized, and centrifuged for 1 min at 10,000 rpm using a microcentrifuge. The supernatant was collected, placed in the NMR tube, and prepared for  $^1\text{H-NMR}$  analysis.

### 2.3. NMR Experiments

<sup>1</sup>H-NMR was carried out using a 500 MHz spectroscopy (JEOL JNM ECZ500R) at a temperature of 25 °C. The parameters used for a total of 128 scans lasting for 10 min included a relaxation delay of 1.5 seconds, X\_angle 60°, and a pre-saturation mode of 4.27 ppm. Subsequently, the deuterated solvent was set as the internal lock, and spectral width was measured from 0 to 10 ppm.

### 2.4. Data Analysis

The <sup>1</sup>H-NMR spectra were analyzed using MestReNova analysis, followed by processing with manual phasing, baseline adjustment, and calibration to internal standard solution signals (TMSP) positioned at the chemical shift of 0.0 ppm. Multiplicities in the observed NMR resonances were labeled according to the convention: s = singlet, d = doublet, dd = doublet of doublets, t = triplet, and m = multiplet [14]. Furthermore, metabolites were identified by comparing the information in the database from previous studies [13-18]. For semi-quantitative analysis, the area of a signal analysis was compared to that of the TMSP signal as an internal standard. All <sup>1</sup>H-NMR signals were normalized to total intensity to develop data for multivariate analysis. MetaboAnalyst software (MetaboAnalyst.ca) was used to analyze multivariate data using Principal Component Analysis (PCA), Partial Least-Squares Discriminant Analysis (PLS-DA), and hierarchical clustering heat map analyses. The spectra were centered and scaled with autoscaling, followed by initial data processing using PCA to evaluate the natural clustering characters. After a clear grouping was observed, the data were subjected to PLS-DA to maximize covariance between measured data (NMR peak intensities) and the response variable (predictive classifications). The PLS-DA coefficient loading plot was used to determine significant metabolites contributing to the separation between the two classes [14]. The model's predictive ability ( $Q^2$ ) was measured using cross-validation, while statistical significance was determined using a permutation test. This was followed by the ranking of the important compounds in the model using variable importance of projection (VIP) scores. A VIP score of >1 indicated that the variable contributed to the variation of the sample. The t-test analysis was used to determine significant differences in metabolites between all samples with p-values  $\leq 0.01$ .

## 3. Results and Discussion

### 3.1. Visual Analysis of <sup>1</sup>H-NMR Spectra

NMR spectroscopy was used as a method to determine the magnetic resonance of molecular nuclei interacting with external magnetic fields [19]. Moreover, NMR could produce a distinct and specific spectrum for each compound, leading to its frequent use in determining the type of metabolite. The quality of the results was determined by the number of compounds identified, rather than signals observed during the NMR analysis [20]. The NMR metabolomics methods have been used widely, making compound identification less complicated. This can be achieved by comparing the signal produced by the samples to those generated by the same compounds in previous reports using CD<sub>3</sub>OD-D<sub>2</sub>O as the solvent [13-18]. Aqueous methanol is commonly used as an extraction solvent alone due to its ability to extract a wide range of compounds, both non-polar and polar. The chemical shift of substances in NMR can be influenced by various solvents. Consequently, multiple reference papers were used to conduct a comparative analysis of potential signal changes that could be identified. In this study, the coupling constant was used as an important parameter to validate the matching signals in the data with the references [15].

The <sup>1</sup>H-NMR spectra were separated into three regions based on their chemical shift ( $\delta$ ), namely the amino acids and terpenoids, carbohydrates, and aromatic compounds. Aliphatic compounds (organic and amino acids) were found in the chemical shift 0.5-3.0 ppm, carbohydrates in 3.1 – 6.0 ppm, and aromatic compounds in > 6 ppm. Furthermore, the various developmental stages of <sup>1</sup>H-NMR spectra of leaves and fruits extracts were analyzed and compared, as shown in Figure 2.

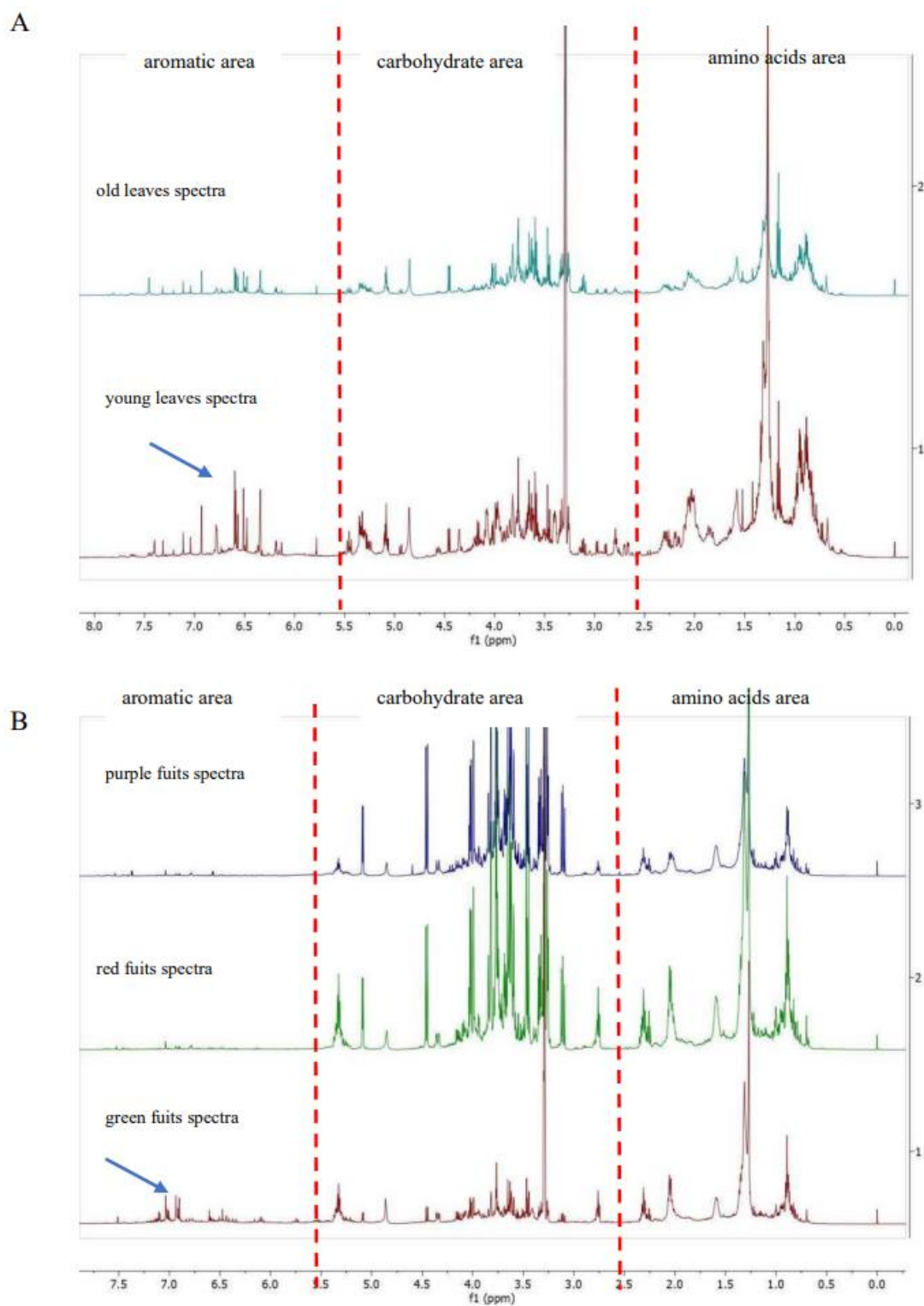


**Figure 2.** The comparison of the  $^1\text{H}$ -NMR spectrum ( $\delta$  0.00–8.00 ppm) indicates signals of *Rhodomyrtus tomentosa* from (A) leaves and (B) fruits of *R. tomentosa*. The arrow shows the aromatics regions which observed differences in signal intensities.

### Metabolomics profiling of *Rhodomyrtus tomentosa*

The results of the putative compounds identified by  $^1\text{H-NMR}$  showed the presence of primary and secondary metabolite compounds. Specifically, the primary metabolites included amino acids (chemical shift 2.0-0.5 ppm) and carbohydrates (chemical shift 5.0-3.0 ppm), with aromatic compounds (chemical shift > 6 ppm) being the secondary metabolites. In the aromatic regions of the NMR spectra, a gradual decrease in phenolic content was observed during leaves and fruits growth. The intensities of signals in the aromatic area in the young leaves and green fruits samples were higher than in the old, red, and purple leaves, as illustrated in Figures 2A and B.

#### 3.2. Identification of Metabolites/Assignment of $^1\text{H-NMR}$ Signals

The advantages of using  $^1\text{H-NMR}$  have been shown in various metabolomics studies. However,  $^1\text{H-NMR}$  presented a significant challenge in chemical identification due to overlapping signals in multiple regions, particularly at 5.0-3.0 ppm, which corresponded to sugar compounds. This caused the inability to identify signals in the sugar region, except for glucose and sucrose, leading to a decrease in the number of substances detected in this study. The results also showed the identification of 20 putative compounds based on the  $^1\text{H-NMR}$  spectra, as presented in Table 1. In the amino acid region, the specific signals of leucine, glutamate, methionine, and aspartate were identified, with chemical shifts ranging from 3.0-0.5 ppm. The organic acid compounds, such as malic, fumaric, and succinic acids were observed in the chemical shifts of between 3.0 - 2.0 ppm. The frequently identified sugars, including mannitol,  $\beta$ -glucose,  $\alpha$ -glucose, and sucrose were also observed at 5.00 - 3.50 ppm. In the less crowded regions, several phenolics were identified, including gallic acid, myricetin, myricetin 3-*O*-rhamnpyranoside, quercetin-3-*O*-glucoside, quercetin, and syringic acid (chemical shifts 10.0 - 6.0 ppm). The remaining compounds identified were  $\alpha$ -linolenic acid, choline, and sterols.

**Table 1.**  $^1\text{H}$  NMR chemical shifts ( $\delta$ ) and coupling constants (Hz) of putative metabolites of *Rhodomyrtus tomentosa* leaves and fruits extracts in MeOH- $d_4$ .

No	Compound	Chemical shifts $\delta$ (ppm) and coupling constants (Hz)
<b>Amino Acids</b>		
1	Aspartate	2.68 (dd, J= 3.0; 17.0 Hz)
2	Glutamic acid	2.06 (m); 2.34 (m)
3	Leucine	0.93 (d, J= 6.85 Hz); 0.98 (d, J= 5.92 Hz)
4	Methionine	2.16 m ; 2.79 (t, J= 6.08; 6.08 Hz)
<b>Organic Acids</b>		
5	Fumaric acid	6.51 (s)
6	Malic acid	4.34 (dd, J= 6.6 ; 4.7 Hz)
7	Succinic acid	2.54 (s)
<b>Sugars</b>		
8	Mannitol	3.77 (d, J= 3.28 Hz)
9	$\beta$ -glucose	4.45 (d, J= 7.79 Hz)
10	$\alpha$ -glucose	5.09 (d, J= 3.84 Hz)
11	Sucrose	5.35 (d, J= 3.91 Hz)
<b>Aromatics Compounds</b>		
12	Gallic acid	7.03 (s)
13	Myricetin	6.34 (d, J= 1.99 Hz); 7.32 (s)
14	Myricetin 3- <i>O</i> -rhamnpyranoside	6.93 (s)
15	Quercetin-3- <i>O</i> -glucoside	6.18 (d, J= 2.08 Hz); 6.37 (d, J= 2.04 Hz)
16	Quercetin	6.13 (s); 7.63 (d, J= 2.22 Hz); 7.51 (s)
17	Syringic acid	3.88 (s)
<b>Other compounds</b>		
18	$\alpha$ -Linolenic acid	1.16 (t, J=7.04 ; 7.04); 1.29 (m)
19	Choline	3.25 (s)
20	Sterol	0.70 (s)

s= singlet, d= doublet, dd= double doublet, t= triplet, m= multiplet

### 3.2. Multivariate Data Analysis

Multivariate PCA was performed to assess the variations of compounds present in fruits and leaves of *R. tomentosa*. The PCA score plot was used to show the separation of classes, while the correlation between variables was interpreted in the loading plot [21]. MetaboAnalyst 5.0 automatically generated five PCs representing 87.6% of all observed variants. Subsequently, the 2D score diagram derived from PC1 and PC2 distinguished fruits and leaves samples. As shown in Figure 3A, the  $Q^2$  cumulative of PC1 and PC2 yielded 57.6% of variants, which was above 50%, indicating a reliable model. PLS-DA was implemented in multivariate analysis to enhance separation, where PC1 and PC2 accounted for 35% and 21.7% of the observed variants, respectively, for a total of 56.7%  $Q^2$  in the 2D score plot. On the PLS-DA score plot presented in Figure 3B, samples of leaves and fruits were positioned in the negative and positive regions of PC1, respectively,

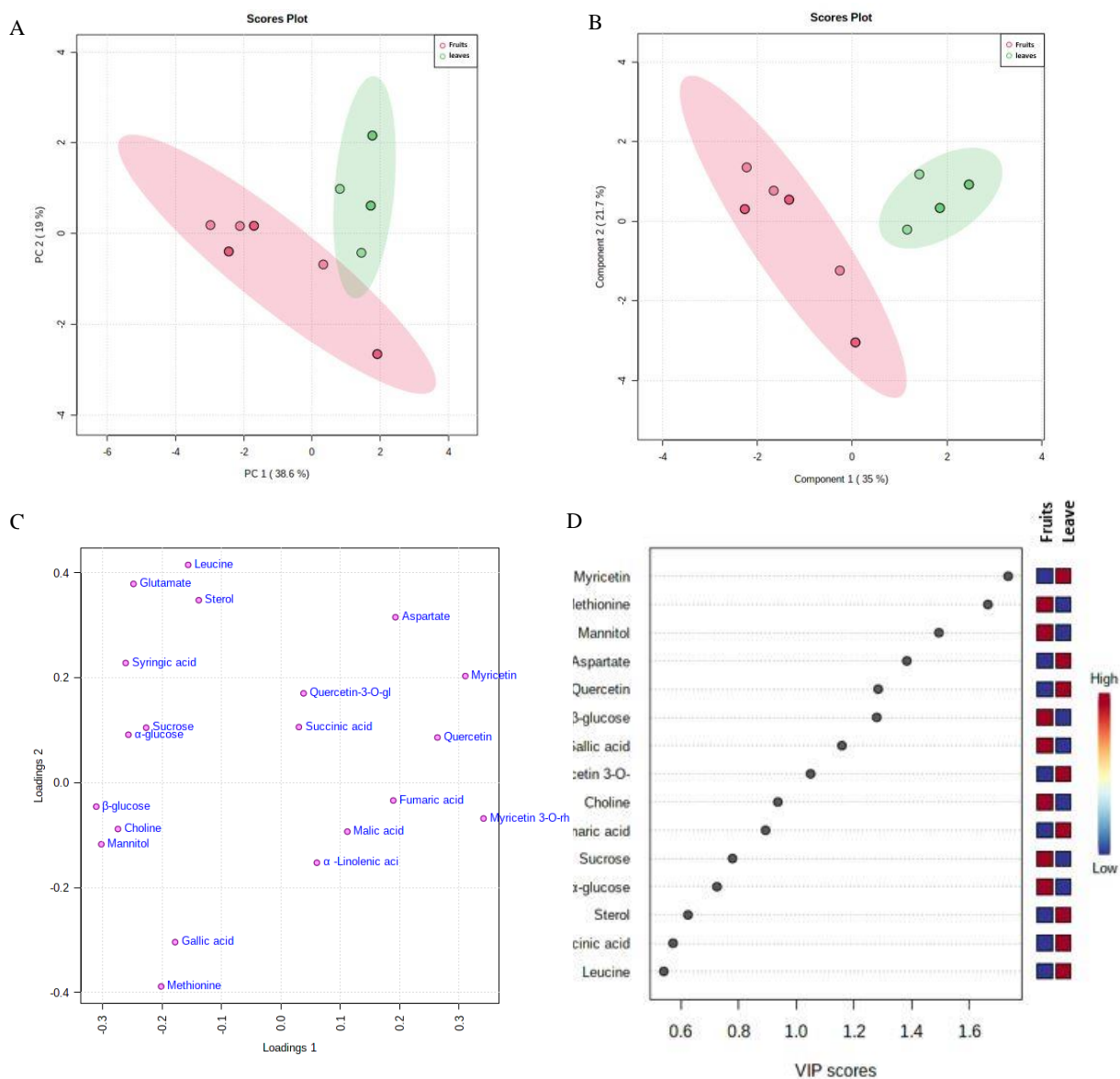


**Figure 3.** Multivariate data analysis of *Rhodomyrtus tomentosa* leaves and fruits samples (A). PCA Score Plot; (B). PLS-DA score plot; (C). PLS-DA loading plot analysis; (D). Variables important in projection (VIP) based on PLS-DA.

### Metabolomics profiling of *Rhodomyrtus tomentosa*

Cross-validation was used to determine the  $Q^2$ , which assessed the predictability of the PLS-DA model. When  $R^2 = 1$  and  $Q^2 = 1$ , the model could precisely describe and predict the data [22]. In this study, PLS-DA showed distinct separation ( $R^2 = 1$ ) and excellent predictability ( $Q^2 = 0.9$ ). The PLS-DA model with a CV-ANOVA less than 0.05 was determined to be the most accurate through 20 permutation tests that validated the results, indicating the reliability of the model [20].

After a separation between leaves and fruits of *R. tomentosa* was observed, a loading plot was used to identify the compounds that distinguished the two groups. Among the 20 compounds observed, Figure 3C showed that there were five distinct components in leaves profile with fruits, as illustrated in Table 1. Compounds observed in the positive region of PC1 were fumaric acid, myricetin, myricetin 3-*O*-rhamnopyranoside, quercetin, and aspartate.

During the implementation of PLS-DA, the VIP score was readily available, reflecting the significance of the model's variables. The VIP was recognized as an instrument for identifying the variables that contributed mainly to the examined variants. Moreover, a VIP score greater than one was frequently used as a selection criterion [23]. As shown in Figure 3D, the score graph indicated that nine metabolites, including myricetin, myricetin 3-*O*-rhamnopyranoside, quercetin, aspartate, choline, gallic acid, methionine, mannitol, and  $\beta$ -glucose, had values greater than 1.

These results suggested the need for further study beyond VIP score compounds to determine when there were notable variations in the chemical composition of fruits and leaves of *R. tomentosa* at the compound level. Subsequently, concentration determination was carried out using a semi-quantitative examination of the compound signal obtained from the internal signal of the TMSP standard. Analysis of signal integration results was conducted using independent t-tests.

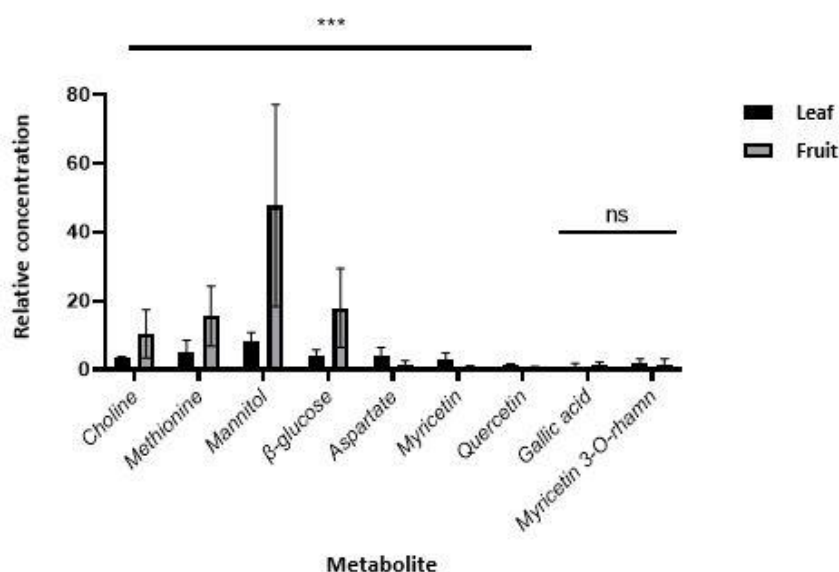


**Figure 4.** Comparison of metabolite concentrations as major contributors to differences between the leaves and the fruits of *Rhodomyrtus tomentosa*

A heatmap was used to assess further differences in the diversity of compound content between fruits and leaves. The concentration of compounds found in fruits and leaves of *R. tomentosa* was visualized through cluster analysis [24]. Heatmap was a form of visualization method that represented data distribution through color changes. In this study, the relative concentrations of compounds in fruits and leaves of *R. tomentosa* served as the data for heatmap analysis, as presented based on the groups of samples. The results showed that the compounds identified showed high diversity and varied concentration, as shown in Figure 5.

Young leaves and green fruits appeared in the same cluster on the heatmap, while some compounds had higher concentrations compared to others. Compounds such as malic acid,  $\alpha$  linolenic acid, aspartate, quercetin 3-*O*-glucoside, fumaric acid, myricetin 3-*O*-rhamnopyranoside, myricetin,

quercetin, methionine, and gallic acid were indicated by a dark brown color. Meanwhile, old leaves, red, and purple fruits had a lower concentration, as indicated by light brown to dark blue colors. Quercetin 3-*O*-glucoside, myricetin 3-*O*-rhamnpyranoside, myricetin, quercetin, and gallic acid compounds were members of the flavonoids group. This was in accordance with the total flavonoids content and the value of the antioxidant capacity of green fruits and young leaves, which were higher than old leaves, red, and purple fruits in a previous study [11]. Based on the results, the total flavonoid content of green fruits was  $95.731 \pm 5.42$  mg QE/g DW and the value of antioxidant capacity was  $1419.75 \pm 3.48$   $\mu$ mol TE/g DW. The young leaves had a total flavonoid content of  $96.375 \pm 3.96$  mg QE/g DW and an antioxidant capacity value of  $1069.38 \pm 6.57$   $\mu$ mol TE/g DW. The total flavonoid and antioxidant capacity values of old leaves were  $70.311 \pm 5.22$  mg QE/g DW and  $844.91 \pm 5.72$   $\mu$ mol TE/g DW, red fruits had  $88.125 \pm 2.72$  mg QE/g DW and  $263.93 \pm 1.60$   $\mu$ mol TE/g DW, while purple fruits  $67.115 \pm 2.57$  mg QE/g DW and  $127.49 \pm 0.57$   $\mu$ mol TE/g DW, respectively [11].

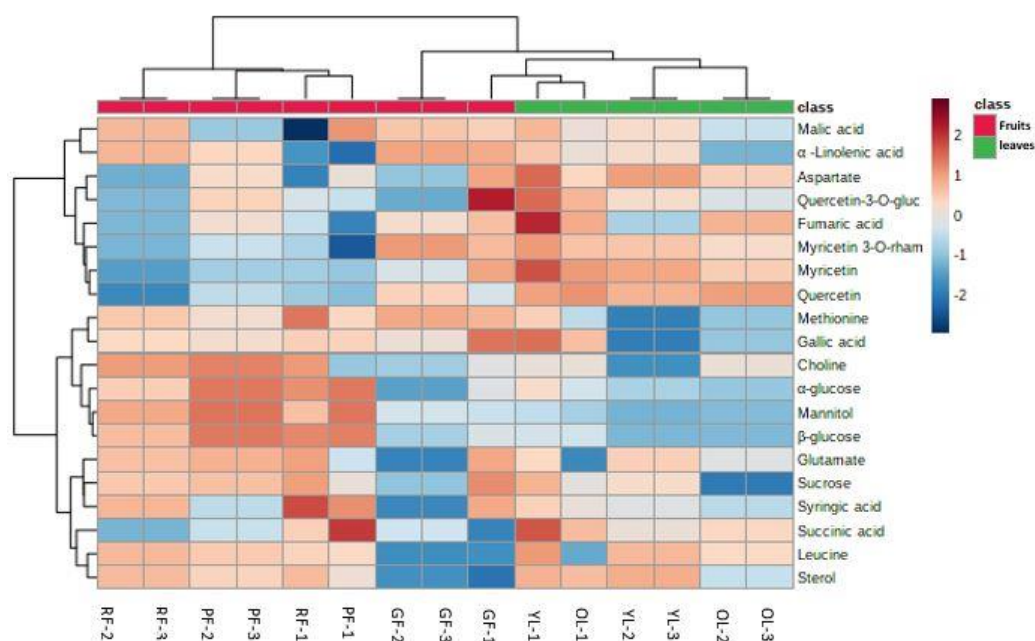


**Figure 5.** Heatmap of leaves and fruits of *Rhodomyrtus tomentosa*. The blue color represents low concentration and the brown color represents high concentration. Note: YL (young leaves), OL (old leaves), GF (green fruits), RF (red fruits), PF (purple fruits)

The number of hydroxycinnamates, caftaric, coumaric acid, and quercetin glucoside compounds in the phenol and flavonoid families increased in grapes (*Vitis* spp.) during the final stages of green fruits development and significantly declined after ripening [16]. Young leaves in *Carica papaya* L. had the highest phenol, flavonoid, and antioxidant activity, followed by mature leaves and seeds [13]. Furthermore, immature wild edible fruits contained significant quantities of polyphenols, including flavonoid [25], indicating that the pre-ripening period served as a defense mechanism for fruits against various congenital diseases. The presence of higher amounts of antioxidants in the unripe fruits of *Rubus ellipticus* and *Myrica esculenta* was consistent with this observation. Based on these results, as fruits ripened, phenols and flavonoids oxidized, participating in the biosynthesis of anthocyanins, which accumulated during maturation, leading to a decrease in flavonoid concentration.

This study elaborated on a previous study focusing on the antioxidant capacity, total flavonoid content, and compound distribution in *R. tomentosa* using histochemical analysis. The antioxidant activity evaluation using FRAP and DPPH showed a comparable proportion, particularly in the green fruits ethanol extracts, indicating the highest FRAP value of  $1367.59 \pm 9.12$   $\mu$ mol TE/g DW and DPPH radical scavenging ability value of  $1419.75 \pm 3.48$   $\mu$ mol TE/g DW. The lowest antioxidant activity was observed in the purple fruits with FRAP value of  $138.38 \pm 1.13$   $\mu$ mol TE/g DW and DPPH of

### Metabolomics profiling of *Rhodomyrtus tomentosa*

127.49±0.57 µmol TE/g DW. As a comparison, the DPPH value of the purple fruits was almost four times lower than the activity antioxidant ORAC value of 431.17±14.5 µmol TE/g DW [4] but higher than another study [26], which was measured in a variety of consumed fruits such as grape, kiwifruit, oranges, apples, mangoes, blueberries, bananas, and blackberries 8.79–92.60 µmol TE/g DW [27].

NMR experiments were carried out to identify and confirm the presence of a wide variety of metabolites in all three samples, namely seed, skin, and pericarp, obtained from *Momordica charantia* fruits [28]. To identify the metabolic differences between these samples, a multivariate statistical analysis was conducted. Different parts of fruits showed significantly varying concentrations of important metabolites, where the highest total flavonoid and phenolic contents were found in seeds and pericarp, followed by skin. Flavonoids metabolites synthesized from naringenin and identified included luteolin, catechin, kaempferol, quercetin, and myricetin. Based on metabolic analysis, the pericarp and seeds contained higher antioxidant activities compared to the skin. The scavenging effects of methanol extracts of ripe fruits measured by DPPH assay were arranged as seed > pericarp > skin [28].

According to the heatmap presented in Figure 5, red and purple fruits belonged to the same cluster. The results showed that the choline, mannitol, β-glucose, α-glucose, and sucrose compounds had a higher concentration, as indicated by a dark brown color. Meanwhile, young leaves and green fruits had a lower concentration, which was shown by the light-blue to dark-blue colors. Mannitol, β-glucose, α-glucose, and sucrose were carbohydrates (sugars) compounds. Ali et al. [16] reported that the concentration of glucose and fructose increased during the ripening stage of grapes (*Vitis* spp.).

The growth of grapefruits was similar to *R. tomentosa* fruits, as both passed through a complex series of biochemical and physical changes, including variations in composition, size, color, taste, texture, and pathogen resistance. Generally, the development of grapes could be separated into three phases. During the initial phase (phase I), fruits grew rapidly due to cell division and expansion, accompanied by the biosynthesis of various compounds, including malic, tartaric, hydroxycinnamates, and tannins. These compounds reached a maximum concentration approximately 60 days after flowering. Phase II referred to the growth lag phase, which was often observed 7 to 10 weeks after flowering, characterized by sugar accumulation. In Phase III (ripening), the berries experienced significant changes in morphology and composition, doubling in size. This indicated the onset of color development associated with anthocyanin accumulation in red wine as well as an increased sweetness, particularly in fructose and glucose levels, followed by decreased acidity [16].

The sugar content of fruits was used as an indicator for assessing the level of ripeness and determining the optimal time for harvest. Carbohydrates, particularly sucrose, were produced by the process of photosynthesis in grapevine leaves and transported to fruits through the phloem. During this process, the sugar content passed through alteration after the transfer due to the loss of water. Furthermore, sugar was used as a source of carbon, energy, and a means of modulating the regulation of gene expression. The accumulation of fructose and glucose started during the second phase of fruits growth, followed by a persistent process, incorporating the transportation of monosaccharides through transporters to facilitate the delivery of sugars to cellular organelles [16]. Sugar plays a crucial role in facilitating plant development, providing energy, where fructose and glucose synthesize sucrose as precursors for the formation of organic acids and pyruvate. Throughout the developmental process, there was a significant rise in the concentrations of fructose and glucose [29].

The dark violet, bell-shaped edible berries of *R. tomentosa*, have been traditionally used as folk medicine to treat issues such as dysentery, diarrhea, and traumatic hemorrhage [30]. Additionally, these berries were used in crafting a renowned fermented beverage called "Ruou sim" on Phu Quoc Island in southern Vietnam, maturing to acquire a deep purple color and an astringent taste [3,4,31]. In China, these berries are transformed into delectable pies, jams, and salad additions, playing a significant role in the creation of traditional wines, beverages, jellies, and freshly canned syrups for human consumption. The berries of *R. tomentosa* contain a rich assortment of chemical constituents, including sugars, minerals, vitamins, phenols, flavonoid glycosides, organic acids, amino acids, quinones, and polysaccharides. Furthermore, this plant thrives in subtropical and tropical regions, serving as a valuable source for cultivating novel ingredients that promote health benefits [26].

#### 4. Conclusion

*Rhodomirtus tomentosa* appeared to have played a significant and holistic role in the daily lives of ancient societies, providing medical benefits. Multiple biological activities of this plant, including antifungal, antimicrobial, antimalarial, antioxidant, anti-inflammatory, and osteogenic properties, have been documented. Therefore, it was essential to comprehend the various parts of *R. tomentosa*, such as the leaves and fruits at various phases of maturation, and the metabolic fate of its various classes of compounds. This study demonstrated that the combination of <sup>1</sup>H-NMR and multivariate data analysis enabled the detection of significant differences between the various developmental stages of the leaves and fruits used in this investigation. At various stages of development, the samples contained substantially different amounts of sugar, aromatic compounds, and phenolic compounds. Green fruits and young leaves contained substantial concentrations of phenolics, including quercetin 3-O glucoside, myricetin 3-O-rhamnpyranoside, myricetin, quercetin, and gallic acid. During the final phases, choline, mannitol,  $\alpha$ -glucose,  $\beta$ -glucose, and sucrose concentrations increased. The approach of this study was useful for analyzing a variety of compounds within the *R. tomentosa* metabolome; however, further research with more sensitive analytical instruments may be desirable to provide a thorough examination of the metabolome transformation and metabolism of the fruit and leaf of *R. tomentosa* at different stages of development.

#### Acknowledgments

The authors are grateful to Gadjah Mada University in Yogyakarta, Indonesia, for supporting this study through the RTA Grant 2022.

#### ORCID

Evi Mintowati Kuntorini: [0000-0001-8508-5354](https://orcid.org/0000-0001-8508-5354)

Laurentius Hartanto Nugroho: [0000-0001-7887-6860](https://orcid.org/0000-0001-7887-6860)

Maryani: [0000-0002-4871-3224](https://orcid.org/0000-0002-4871-3224)

Tri Rini Nuringtyas: [0000-0002-8011-8396](https://orcid.org/0000-0002-8011-8396)

#### References

- [1] M. İ. Han and G. Bulut (2015). The folk-medicinal plants of kadişehir (Yozgat – Turkey), *Acta. Soc. Bot. Pol.* **84**(2), 237–48.
- [2] Z. Zhao, W. Lei, X. Jing, F. Ying, T. Jiale, H. Xirui and L. Bin (2019). *Rhodomirtus tomentosa* (Aiton.): A review of phytochemistry, pharmacology and industrial applications research progress, *Food Chem.* **309**, 1–10.
- [3] T. N. H. Lai, H. Marie-France, Q. L. Joëlle, B.T.N. Thi, R. Hervé, L. Yvan, and M. A. Christelle (2013). Piceatannol, a potent bioactive stilbene, as major phenolic component in *Rhodomirtus tomentosa*, *Food Chem.* **138**(2–3), 1421–1430.
- [4] T.N.H. Lai, A. Christelle, R. Hervé, M. Eric, B.T.N. Thi and L. Yvan (2015). Nutritional composition and antioxidant properties of the sim fruit (*Rhodomirtus tomentosa*), *Food Chem.* **168**, 410–416.
- [5] B. Salehi, M. Valussi, A. K. Jugran, M. Martorell, K. Ramírez-Alarcón, Z. Z. Stojanović- Radić and J. Sharifi-Rad (2018). Nepeta species: from farm to food applications and phytotherapy, *Trends F. Sci. Tech.* **80**, 104–122.
- [6] M. Tayeh, S. Nilwarangoon, W. Mahabusarakum and R. Watanapokasin (2017). Anti-metastatic effect of rhodomirtone from *Rhodomirtus tomentosa* on human skin cancer cells, *Int. J. Oncol.* **50**(3), 1035–1043.
- [7] P. Na-Phatthalung, M. Teles, S. P. Voravuthikunchai, L. Tort and C. Fierro-Castro (2018). Immunomodulatory effects of *Rhodomirtus tomentosa* leaf extract and its derivative compound, rhodomirtone, on head kidney macrophages of rainbow trout (*Oncorhynchus mykiss*), *Fish Phys. Biochem.* **44**(2), 543–555.
- [8] A H. Hamid, R. Mutazah, M. M. Yusoff, N. A. Abd Karim and R. A. F. Abdull (2017). Comparative analysis of antioxidant and antiproliferative activities of *Rhodomirtus tomentosa* extracts prepared with various solvents. *Food Chem. Toxicol.* **108**, 451–457.
- [9] I.W. Kusuma, A. Nurul and S. Wiwin (2016). Search for biological activities from an invasive shrub species rosemyrtle (*Rhodomirtus tomentosa*), *Nusantara Biosci.* **8**(1), 55–59.

Metabolomics profiling of *Rhodomyrtus tomentosa*

- [10] J. Saising, M.T. Nguyen, T.Hartner, P. Ebner, A.A. Bhuyan, A. Berscheid and F. Gotz (2018). Rhodomyrtone (Rom) is a membrane-active compound, *Biochim. Biophysic Acta-Biomembranes* **1860**(5), 1114–1124.
- [11] E. M. Kuntorini, L. H. Nugroho, Maryani and T. R. Nuringtyas (2022). Maturity effect on the antioxidant activity of leaves and fruits of *Rhodomyrtus tomentosa* (Aiton.) Hassk, *AIMS Agric. Food* **7**(2), 282–296.
- [12] S. A. Wilde (1977). Munsell color charts for plant tissues. New Windsor, New York, pp 10-15
- [13] N. Gogna, N. Hamid and K. Dorai (2015). Metabolomic profiling of the phytomedicinal constituents of *Carica papaya* L. leaves and seeds by <sup>1</sup>H NMR spectroscopy and multivariate statistical analysis, *J. Pharm. Biomed. Anal.* **115**, 74–85.
- [14] S. Mishra, N. Gogna and K. Dorai (2019). NMR-based investigation of the altered metabolic response of *Bougainvillea spectabilis* leaves exposed to air pollution stress during the circadian cycle. *Environ Exp. Bot.* **164**, 58–70.
- [15] H. K. Kim, H. C. Young and R. Verpoorte (2010). NMR-based metabolomic analysis of plants. *Nat. Protoc.* **5**(3), 536–549.
- [16] K. Ali, M. Federica, M. F. Ana, S. P. Maria, H.C. Young and R. Verpoorte (2011). Monitoring biochemical changes during grape berry development in portuguese cultivars by NMR spectroscopy, *Food Chem.* **124**, 1760–1769.
- [17] T. R. Nuringtyas, H. C. Young, R. Verpoorte, G.L.K. Peter and A. L. Kirsten (2012). Differential tissue distribution of metabolites in *Jacobaea vulgaris*, *Jacobaea aquatica* and their crosses, *Phytochemistry* **78**, 89–97.
- [18] A. Cerulli, M. Milena, M. Paola, H. Jan, P. Cosimo and P. Sonia (2018). Metabolite profiling of ‘green’ extracts of *Corylus avellana* leaves by <sup>1</sup>H NMR spectroscopy and multivariate statistical analysis, *J. Pharm. Biomed. Anal.* **160**, 168–78.
- [19] K. Hatada and T. Kitayama (2004). Basic principles of NMR. In: Hatada K. and T. Kitayama (eds) NMR spectroscopy of polymers. Springer, New York, pp 1– 34.
- [20] K. A. Leiss, H. C. Young R. Verpoorte, and G.L.K. Peter (2011). An overview of NMR-based metabolomics to identify secondary plant compounds involved in host plant resistance. *Phytochem. Rev.* **10**(2), 205–216.
- [21] R. Islamadina, C. Adelin and A. Rohman (2020). Chemometrics application for grouping and determinating volatile compound which related to antioxidant activity of turmeric essential oil (*Curcuma longa* L.), *J. Food Pharm. Sci.* **8**(2), 225-239.
- [22] M N. Triba, L. M. Laurence, A. Roland, G. Corentine, B. Nadia, N. Pierre, N. R. Douglas and S. Philippe (2015). PLS/OPLS models in metabolomics: the impact of permutation of dataset rows on the k-fold cross-validation quality parameters. *Molecular BioSystem.* **11**(1), 13–19.
- [23] M. Farrés, P. Stefan, T. Stefan and T. Romà (2015). Comparison of the variable importance in projection (VIP) and of the selectivity ratio (SR) methods for variable selection and interpretation, *J. Chem.* **29** (10), 528–536.
- [24] J. Xia and D. S. Wishart (2016). Using metaboanalyst 3.0 for comprehensive metabolomics data analysis, *Curr. Prot. Bioinform.* **55**, 1-91.
- [25] T. Belwal, P. Aseesh, D. B. Indra, S. R. Ranbeer and L. Zisheng (2019). Trends of polyphenolics and anthocyanins accumulation along ripening stages of wild edible fruits of indian himalayan region, *Sci. Reports.* **9**(1), 1–11.
- [26] P. Wu, G Ma, N. Li, Q Deng, Y. Yin and R. Huang (2015). Investigation of in vitro and in vivo antioxidant activities of flavonoids rich extract from the berries of *Rhodomyrtus tomentosa* (Ait.) Hassk., *Food Chem.* **173**, 194–202.
- [27] X.Wu, GR Beecher and JM. Holden (2004). Lipophilic and hydrophilic antioxidant capacities of common foods in the united states, *J. Agric. Food Chem.* **52**, 4026–4037.
- [28] S Mishra, Ankit, R Sharma, N Gogn and K Dorai (2020). NMR-based metabolomic profiling of the differential concentration of phytomedicinal compounds in pericarp, skin and seeds of *Momordica charantia* (bitter melon), *Nat Prod Res.* **36** (1), 390–5.
- [25] P. Wang, Z. Linlin, Y. Hongbing, H. Xujie, W. Cuiyun, Z. Rui, Y. Jun and C. Yunjiang (2022). Systematic transcriptomic and metabolomic analysis of walnut (*Juglans regia* L.) kernel to trace variations in antioxidant activity during ripening, *Sci. Horticulturae* **295**, 1-12.
- [30] Salni, H Marisa, LA Repi (2020). Antioxidant activities bioactive compound of ethyl acetate extracts from rose myrtle leaves (*Rhodomyrtus tomentosa* (Ait.) Hassk.). *IOP Conf. Ser. Mater. Sci. Eng.* **857**(1), 1–7
- [31] TS Vo and DH Ngo (2019). The health beneficial properties of *Rhodomyrtus tomentosa* as potential functional food, *Biomolecules* **9**(2), 1–16.